



High pressure photoluminescence of bismuth-doped yttria-alumina-silica glass

Mark A. Hughes, Robert McMaster, John E. Proctor, Daniel W. Hewak, Takenobu Suzuki & Yasutake Ohishi

To cite this article: Mark A. Hughes, Robert McMaster, John E. Proctor, Daniel W. Hewak, Takenobu Suzuki & Yasutake Ohishi (2022): High pressure photoluminescence of bismuth-doped yttria-alumina-silica glass, High Pressure Research, DOI: [10.1080/08957959.2022.2044031](https://doi.org/10.1080/08957959.2022.2044031)

To link to this article: <https://doi.org/10.1080/08957959.2022.2044031>



© 2022 The Author(s). Published by Informa UK Limited, trading as Taylor & Francis Group



Published online: 27 Feb 2022.



Submit your article to this journal [↗](#)



View related articles [↗](#)



View Crossmark data [↗](#)

High pressure photoluminescence of bismuth-doped yttria-alumina-silica glass

Mark A. Hughes^a, Robert McMaster^{a,b}, John E. Proctor^a, Daniel W. Hewak^c, Takenobu Suzuki^d and Yasutake Ohishi^d

^aJoule Physics Laboratory, School of Science, Engineering and Environment, University of Salford, Salford, UK; ^bNanofunctional Materials Group, Department of Materials, University of Manchester, Manchester, UK; ^cOptoelectronics Research Centre, University of Southampton, Southampton, UK; ^dOptical Functional Materials Laboratory, Toyota Technological Institute, Nagoya, Japan

ABSTRACT

We report the effects of high pressure, up to 10.45 GPa, on the photoluminescence of Bi-doped yttria-alumina-silica glass under 532 nm excitation. We identify three emission bands attributed to Bi³⁺, Bi⁺ and a NIR emitting Bi centre, Bi_{NIR}. As the pressure is increased up to ~6 GPa, an irreversible discontinuity in the trend for emission band energies indicates that an irreversible structural modification occurs. This irreversible discontinuity results in the peak energy of emission bands attributed to Bi⁺ and Bi_{NIR} shifting from those typical of Bi-doped oxide glasses to those observed in Bi-doped gallium-lanthanum-sulfide glass. The Bi³⁺ emission band can be almost eliminated at ~6 GPa, but its intensity increases rapidly as the pressure is further increased. The ability we report here to irreversibly modify the emission of Bi-doped glass using pressure treatment adds an extra processing technique to researchers looking to optimize the emission from Bi-doped glasses.

ARTICLE HISTORY

Received 31 March 2021
Accepted 15 February 2022

KEYWORDS

Photoluminescence;
bismuth; glass

1. Introduction

When doped into glasses, bismuth usually generates characteristic absorption bands at ~500, 700, and 850 nm, along with some weaker absorption bands at longer wavelengths. Broad photoluminescence (PL) bands can be readily obtained from Bi-doped glasses, these PL bands are highly dependent on the glass composition, melting conditions and excitation wavelength [1]. The PL bands often cover the technologically useful telecommunications bands, which has sparked interest in using Bi-doped glasses for optical amplifiers and lasers. In 2005, the first Bi-doped fibre laser was demonstrated [2]; since then, developments have been made including tuneable lasing between 1150 and 1550 nm [3], 1389 and 1538 nm [4], 1600 and 1800 nm [5], and output powers of 22 W [4]. However, despite these developments no commercially available Bi-doped amplifier

CONTACT Mark A. Hughes  m.a.hughes@salford.ac.uk  Joule Physics Laboratory, School of Science, Engineering and Environment, University of Salford, Salford M5 4WT, UK

© 2022 The Author(s). Published by Informa UK Limited, trading as Taylor & Francis Group
This is an Open Access article distributed under the terms of the Creative Commons Attribution License (<http://creativecommons.org/licenses/by/4.0/>), which permits unrestricted use, distribution, and reproduction in any medium, provided the original work is properly cited.

or laser has been produced; one of the main reasons for this is that Bi-doped glass lasers suffer from unsaturable losses (losses not originating from the primary absorption transition of the lasing ion), and excited state absorption [6]. Additionally, there is no consensus on the origin of the near-infrared (NIR) emission from Bi-doped glasses, and convincing arguments have been made for the involvement of a variety of different centres, including Bi-metal clusters [7], negatively charged Bi₂ dimers [8,9], point defects [10], Bi⁺ [11], and Bi⁵⁺ [12,13]. Red emission from Bi-doped glasses is also often observed; however, this is usually ascribed to Bi⁺, Bi²⁺ or Bi³⁺ with a relatively high degree of certainty.

Glass processing methods for controlling the presence of red and NIR emitting centres are also not well understood, this means that progress has largely been made through trial and error modifications to glass composition and melting conditions; however, the addition of SiC to Bi-doped germanate glass melts can enhance NIR emission bands [14]. One approach to tackle these problems which has not been attempted to date is to study the behaviour of the observed PL under high pressure. This method can allow us to obtain information to assist in understanding the origin of the PL, from studying the shifts in peak wavelength, width and intensity of PL upon pressure change. In addition, high pressure has the potential to irreversibly modify the structure of the host material to improve its optical and PL properties.

In this study, we report the first high pressure PL measurements of a Bi-doped glass by using a diamond anvil cell (DAC). As pressure is increased, the PL bands from Bi:YAlSi switch rapidly at ~6 GPa from those usually observed in Bi-doped oxide glasses, to those observed in a Bi-doped chalcogenide. The modified PL bands remain as the pressure is reduced to ambient and are still present at least two years after pressure treatment.

2. Experimental

2.1. Glass melting

We fabricated three Bi-doped oxide glasses. These were Bi:YAlSi, with a composition (mol.%) of 62SiO₂:22.5Al₂O₃:13Y₂O₃:2.5Bi₂O₃, which was melted at 1550°C for 60 min [15]; Bi:LiAlSi, with a composition (mol.%) of 13Li₂O:23Al₂O₃:63.5SiO₂:0.5Bi₂O₃, which was melted at 1600°C for 120 min [16]; and Bi:PbZnAlGe, with a composition (mol.%) of 74.4GeO₂:10ZnO:6Al₂O₃:6PbO:0.6Bi₂O₃, which was melted at 1250°C for 30 min [17]; these glass melts were quenched by pouring them onto stainless steel plates preheated to 600°C.

A Bi-doped chalcogenide glass, Bi:GaLaS [1], with a composition of 70Ga₂S₃:23La₂S₃:6La₂O₃:1Bi₂S₃, was fabricated by batching components into a vitreous carbon crucible inside a glove box then transferring to the furnace. Ga₂S₃ and La₂S₃ were dehydrated and purified and in a dry-argon purged furnace to reduce OH⁻ impurities. The lanthanum oxide and bismuth sulphide were purchased commercially and used without further purification. The glass was melted at 1150°C for 24 h, in a silica tube furnace with a constant argon flow of 0.5 litres per minute before being quenched in a water jacket and annealed at 400°C for 12 h. All glass was cut and polished into slabs ~2 mm in thickness. These glasses were selected from our previous studies of Bi-

doped oxide and chalcogenide glasses under NIR excitation for investigation with green excitation and high pressure.

2.2. High pressure spectroscopic measurements

High pressure measurements were performed on a sample of Bi:YAlSi. A homemade electrical discharge machine [18] was used to create a $\sim 100\ \mu\text{m}$ diameter hole in a stainless steel foil gasket (200 μm thickness, 56–60 μm thickness after preindentation). A $\sim 50\ \mu\text{m}$ shard was chipped from a Bi:YAlSi polished slab and placed inside the hole in the gasket, which was placed between the culets of the DAC (450 μm diameter culets, type 1a natural diamonds selected for low fluorescence). NaCl was utilized as a pressure-transmitting medium, providing quasi-hydrostatic conditions for the pressures attained in this study at ambient temperature [19]. Care was taken to ensure that the Bi:YAlSi sample was surrounded on both sides by NaCl instead of being pressed directly against the culet of one of the diamonds. Pressure was measured using the PL signal from a small chip of Samarium-doped Yttrium Aluminium Garnet (Sm:YAG) placed in the sample chamber close to the Bi:YAlSi sample, using the calibration from ref [20]. Sm:YAG was utilized in preference to the more commonly used ruby PL scale since the Sm:YAG PL lies at a shorter wavelength than the ruby PL, so does not overlap with that from the Bi:YAlSi sample.

PL spectra were obtained using a custom-built optical spectrometer described previously [21]. This consisted of narrow linewidth 532 nm laser excitation and a conventional single grating (300 lines per mm) 0.32 m Horiba iHR320 with spectrometer with Symphony LN2 cooled silicon CCD. Laser line rejection filters passed emission to within $200\ \text{cm}^{-1}$ of the laser line. The PL spectra of Sm:YAG were collected on the same system, but utilizing a 1200 lines per mm grating. The spectra were collected using a $100\ \mu\text{m}$ width entrance slit, giving a resolution of $2.5\ \text{cm}^{-1}$.

All ambient pressure PL measurements were performed using the same excitation laser and detection system as the high pressure measurements; however, the full range of the NIR PL from the Bi-doped glasses is limited by range of our CCD detector. The full range of the NIR PL from these Bi-doped glasses can be seen elsewhere for Bi:YAlSi [15], Bi:LiAlSi [16], Bi:PbZnAlGe [17] and Bi:GaLaS [1]. Absorption spectra were performed on polished bulk glass samples using a Perkin-Elmer, Lambda 900 double-beam spectrophotometer. Raman signals from the Bi-doped glasses could not be resolved because of the proximity of the PL signal to the excitation wavelength.

3. Results and discussion

Figure 1 shows the absorption spectrum of 2.5% Bi-doped YAlSi glass. Broad absorption bands at 500 and 700 nm, characteristic of Bi-doped glasses, can be clearly observed. The absorption spectrum of undoped YAlSi glass is also shown. A red shift in the band edge of the Bi-doped glass in comparison to the undoped glass suggests the presence of an absorption band obscured by the band edge at $\sim 330\ \text{nm}$, which has been reported in Bi-doped materials [22]. The inset shows a close-up of the low absorption region. A comparison to the undoped glass highlights a weak tail of an absorption band at $\sim 1000\ \text{nm}$, we observed a similar absorption band in Bi-doped germanate glass [23]. We also observed an 800 nm absorption band in Bi-doped germanate glass, which we proposed

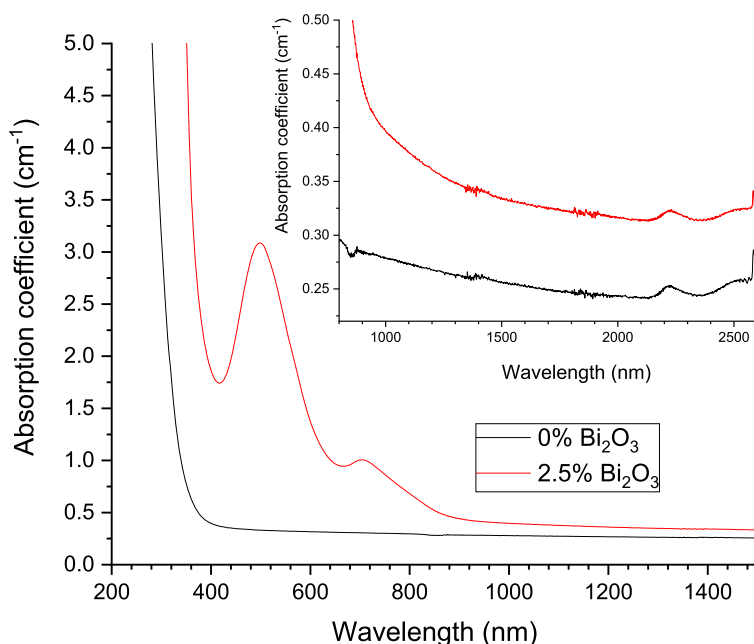


Figure 1. Absorption spectra of 2.5 mol.% Bi_2O_3 doped YAlSi glass and undoped YAlSi glass.

was associated with a different Bi-related centre to the 500, 700 and 1000 nm absorption bands; however, there is no evidence of the 800 nm absorption band in Bi:YAlSi, suggesting the additional Bi centre is not present in Bi:YAlSi.

Figure 2 shows the PL spectra from Bi:YAlSi, Bi:LiAlSi, Bi:PbZnAlGe and Bi:GaLaS at ambient pressure, as well as the PL spectrum from Bi:YAlSi at the maximum pressure of 10.45 GPa. All the spectra were deconvoluted into Gaussians; the peak centre, width and area of the Gaussian function were optimized in the fitting procedure and we used a dynamic fitting algorithm that searched 400 initial parameter values. The number of Gaussians used in the fit was determined by the minimum number required to give a coefficient of determination (R^2) > 0.995, which was three in all cases. These three Gaussians are labelled 1–3. Gaussians 2 and 3 cover the relatively well established Bi centres that emit in the visible. Bi^{3+} and Bi^{2+} emit visible, but no NIR luminescence. In various crystals, Bi^{3+} can give rise to emission from UV to ~ 550 nm [24–26] and 650 nm in Y_2WO_6 [27]. Due to the high covalency of its lattice site, Bi^{3+} doped ZnWO_4 can give rise to PL at 665 nm [28]. The red PL from Bi-doped glass has previously been assigned to Bi^{2+} [29–31]; however, it was recently shown, using magnetic circular dichroism measurements, that the red PL from Bi-doped pure silica glass does not originate from Bi^{2+} [32]. This suggests that Gaussian 3, which peaks at 630–680 nm originates from Bi^{3+} , and can be attributed to the $^3\text{P}_1 \rightarrow ^1\text{S}_0$ transition of Bi^{3+} [33]. The energy of the Gaussian 2 peak is too low for any reports of emission from Bi^{3+} , other possibilities include Bi^0 and Bi^+ . By comparison to the energy level models of these centres [34–36], Gaussian 2 most likely originates from Bi^+ . Gaussian 1 is outside the range of the well-established Bi centres emitting in the visible and into the wavelength range assigned to the controversial NIR emitting Bi centre. Unfortunately, our detection system could not detect beyond 1100 nm,

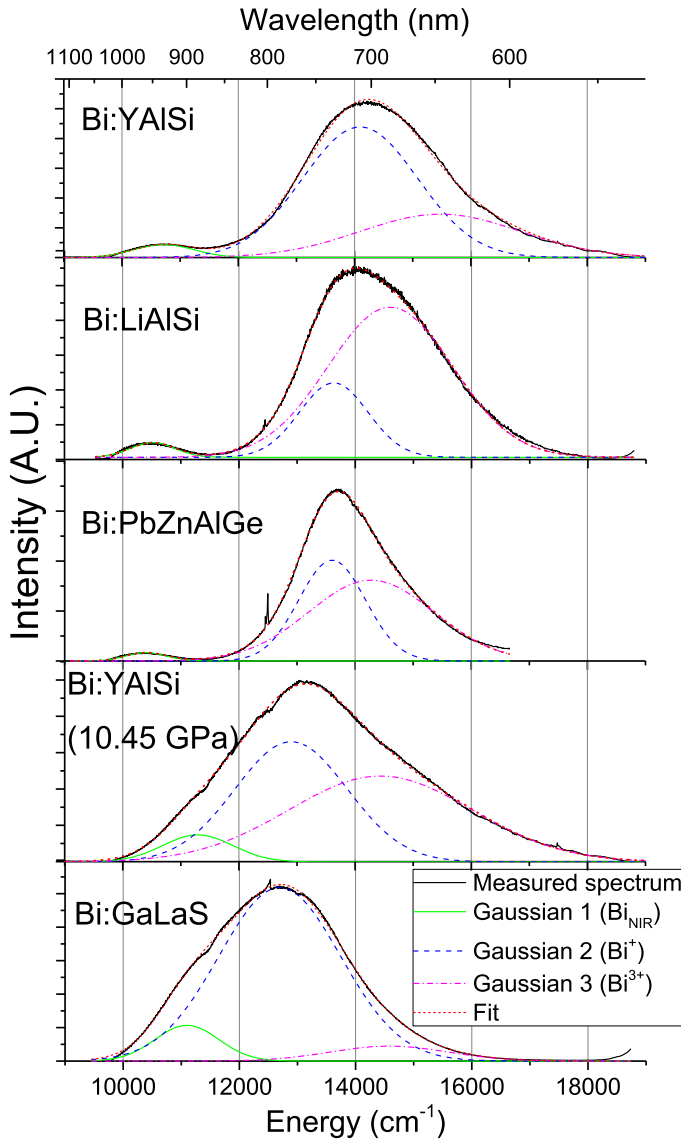


Figure 2. PL spectra, deconvoluted into three Gaussians, of Bi:YAlSi, Bi:LiAlSi, Bi:PbZnAlGe and Bi:GaLaS at ambient pressure, as well as Bi:YAlSi at 10.45 GPa. The proposed origin of each Gaussian band is shown. Excitation was at 532 nm.

whereas the NIR Bi emission is usually reported as peaking between 1100 and 1500 nm, so it is possible only a portion of this emission band has been detected.

In previous work we attributed the optically active centre in Bi:YAlSi to Bi₂ dimers produced by a second order reaction of the kind: $2\text{Bi} \rightarrow \text{Bi}_2$, based on the quadratic dependence of absorption strength (α) on Bi doping concentration ($[\text{Bi}]$) *i.e.* $\alpha = k[\text{Bi}]^2$, where k is a constant [15]. However, this only refers to absorbing Bi centres and doesn't determine if they are emitting centres. Later, we found that a more general model relating α to $[\text{Bi}]$: $\alpha = k[\text{Bi}]^x$, where the power law factor, x , varies between 0.54 and 2.76, depending on the glass

composition [37]. This observation is yet to be fully explained and further complicates the determination of the NIR emitting Bi centre, here we refer to this centre as Bi_{NIR} .

Further examination of Figure 2 shows that the position and relative intensities of Gaussians 1 and 2 fall into two categories: Bi:YAlSi, Bi:LiAlSi, Bi:PbZnAlGe oxide glasses have Gaussian 1 peaks at $\sim 10,500 \text{ cm}^{-1}$ (may peak at lower energy because of its proximity to the detector cut-off), and Gaussian 2 peaks at $\sim 13,800 \text{ cm}^{-1}$; whereas in Bi:YAlSi at 10.45 GPa and Bi:GaLaS have Gaussian 1 peaks at $\sim 11,200 \text{ cm}^{-1}$ (well within the detector range) and Gaussian 2 peaks at $12,800 \text{ cm}^{-1}$. This shows that Bi-doped oxide and chalcogenide glasses have different PL characteristics, but under high pressure, the PL characteristics of Bi:YAlSi shift from those typical of oxide glasses to those typical of chalcogenide glasses. Gaussian 3 doesn't fit in this categorization; however, the relative weakness of Gaussian 3 in the Bi:GaLaS PL spectrum is likely due to the GaLaS bandedge at $\sim 600 \text{ nm}$ and the strong Bi absorption at $\sim 500 \text{ nm}$ could affect the strength and position of Gaussian 3 in all glasses.

Figure 3(a) shows a contour plot representing the PL from Bi:YAlSi with the completed pressure treatment given taking the pressure from ambient up to 10.45 GPa then back down to ambient in increments of 0.5–2 GPa. Example spectra are given in Figure 3(b). It can be seen that as the pressure is increased, the PL intensity decreases steadily until $\sim 6 \text{ GPa}$ is reached, then as pressure is increased further, there is a sudden broadening and rapid increase in PL intensity which reaches a maximum at the maximum pressure reached; the PL peak has also shifted to $\sim 1000 \text{ cm}^{-1}$ lower energy. As the pressure decreases the PL intensity decreases steadily, but keeps the same peak energy reached at high pressure even down to ambient, showing a metastable change in the emission characteristics of Bi:YAlSi with pressure treatment.

Figure 4(a) shows peak areas of the fitted Gaussians (1, 2 and 3). As the pressure is increased from ambient all the Gaussians display a reduction in intensity; however, the reduction for Gaussian 3, attributed to Bi^{3+} , is far more dramatic than the other Gaussian bands and the contribution from Gaussian 3 is almost zero at 6 GPa. This elimination of the Bi^{3+} emitting band is very important since the presence of other emitting and

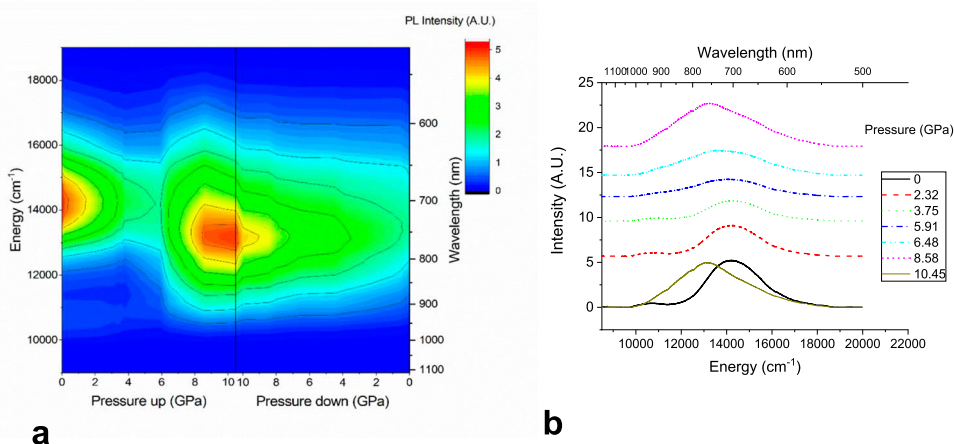


Figure 3. (a) Contour plot of the PL spectra of Bi:YAlSi as a function of increasing, then decreasing, pressure. (b) Example PL spectra at various increasing pressures.

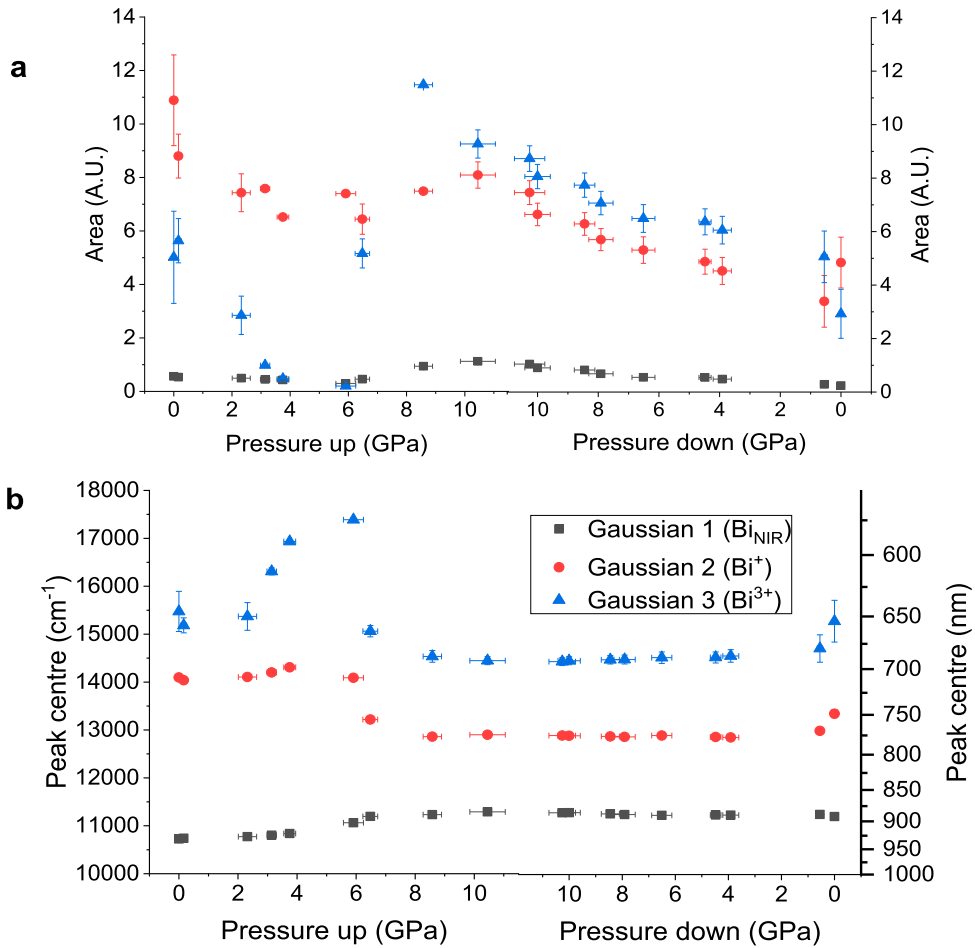


Figure 4. (a) Area and (b) peak centre of the Gaussians 1, 2 and 3 determined from deconvolution of the PL spectra of Bi:YAlSi, as a function of increasing, then decreasing, pressure.

absorbing centres must be detrimental to efforts to make an efficient broadband laser or amplifier using the Bi_{NIR} centre.

Glass modifiers can have an opposite effect since by adding antimony oxide as an oxidation agent to a bismuthate glass, NIR emission centres can be eliminated and Bi³⁺ is formed [38]. Gaussian 1, assigned to the technologically useful Bi_{NIR} centre, doubles in intensity compared to ambient when the maximum pressure of 10.45 GPa is reached, this trend is reversed as the pressure is brought back to ambient.

As shown in Figure 4(b), the peak of Gaussian 3 increases in energy by ~ 2500 cm⁻¹ as it is decreasing in intensity. As shown in Figure 4(a), the intensity of Gaussian 3 is around zero at 6 GPa, but its intensity increases rapidly with further pressure increase until it is the most intense emission band at 8.5 GPa. Gaussian 3 then decreases steadily in intensity as the pressure is increased to 10.45 GPa then back down to ambient.

The pressure dependence of spin-allowed electronic transitions in transition metal ion-doped crystals [39,40] and glasses [41] is well reported in the literature. The continuous blue shift usually observed with increasing pressure is well described by the crystal

field model where hydrostatic pressure increases the crystal field strength and/or changes symmetry by compression of ion-ligand bonds. In contrast, luminescence from the narrow spin forbidden electronic transitions in transition metal ion tend to exhibit a continuous red shift with increasing pressure due to a small decrease in the Racah B parameter with pressure and consequently an increase in the degree of covalency of the ion-ligand bond [42,43]. In rare earth doped materials $f \rightarrow f$ luminescence transitions also tend to display a continuous red shift with increasing pressure again due to covalency effects [43]. In Figure 4(b), up to the discontinuity at ~ 6 GPa, all the Gaussian bands display a blue shift, which suggests that this can be explained by a pressure-induced increase in crystal field strength.

The discontinuity in the trend for peak areas and energies that occurs at 6 GPa, and its irreversibility indicates that an irreversible structural modification occurs at this pressure. A discontinuity in the trend of the emission from Cr^{3+} doped sodium silicate glasses, which was also irreversible with decompression has been reported to occur at ~ 9 GPa [41]. This was attributed to a change in the O coordination of Si from 4-fold to 5- or 6-fold. A change in the coordination of Si was also reported to occur in sodium silicate glasses quenched at pressures between 4 and 6 GPa in quenched melts; this was determined by NMR, Raman and IR measurements [44]. We, therefore, propose that a similar structural modification occurs in Bi:YAlSi at ~ 6 GPa, which may be an increase in Si coordination. We refer to the initial structure of Bi:YAlSi as phase 1 and the metastable final structure as phase 2. At 6 GPa, the structural modification causes emission bands attributed to Bi^+ and Bi^{3+} (Gaussians 2 and 3) to shift to lower energy, whereas the Bi_{NIR} band shifts to higher energy. This indicates that the Bi_{NIR} centre is located at a different site in the glass lattice to the Bi cations. The observed shift to lower emission energy for the Bi cations is consistent with an O coordinated site, since the proposed increase in O coordination of Si in phase 2 could decrease the O coordination of other sites and reduce their crystal field strength. The Bi_{NIR} centre could be situated at another site which increases in O coordination in phase 2, but not enough is known about the structure of YAlSi glass to be more specific. This understanding of how pressure related effects on Bi doped silicate glasses, such as a change coordination of Si, affect the emission peaks and intensities of the various Bi centres could assist in the formulation of Bi doped silicate glasses for a required emission wavelength and intensity if, for instance, a particular glass modifier is known to increase the coordination of Si of that glass.

To the best of our knowledge there are no reports of the pressure dependence of Bi luminescence apart from a Bi^{3+} to V charge transfer luminescence in Bi-doped YVO_4 [45].

Chalcogenide glasses display a persistent p-type conductivity that cannot be reversed with standard donor dopants; however, doping with high concentrations of Bi (5–10 at.%) is one of the only know methods for reversing the carrier type in chalcogenide glasses. The Bi centre responsible for this carrier type reversal (CTR) is controversial and we have proposed that the Bi centre that causes CTR in chalcogenide glasses is the same Bi centre that causes the controversial NIR luminescence from Bi-doped glasses [37]. We have also demonstrated that implantation of Bi into chalcogenide glasses, including GaLaS, can cause carrier type reversal at much lower Bi concentrations than melt doped chalcogenide glasses [46]. We also proposed that the centre responsible for CTR was Bi^+ or Bi^{2+} [46], which is consistent with Bi^+ being the dominant centre in the PL spectrum of Bi:GaLaS in Figure 2.

4. Conclusions

An irreversible discontinuity in the trend of emission from Bi:YAlSi as pressure is increased occurs at ~ 6 GPa, which is attributed to an irreversible structural modification of the YAlSi glass that may consist of an increase in Si coordination. After the pressure treatment, emission bands attributed to Bi^+ and Bi^{3+} display an irreversible shift to lower energy, whereas the emission band attributed to the Bi_{NIR} centre displays an irreversible shift to higher energy, indicating that it has a different lattice site to the Bi cations. Also after pressure treatment, the peak energy of emission bands attributed to Bi^+ and the Bi_{NIR} centres shifted from those typical of Bi-doped oxide glasses to those observed in a Bi-doped chalcogenide glass. Emission from Bi^{3+} can be almost eliminated at ~ 6 GPa, although in our particular pressure treatment this was not irreversible. The ability to irreversibly change the emission bands of Bi-doped glass using pressure treatment adds a potential extra degree of freedom in the processing parameters for the control of centres in Bi-doped glasses.

CRedit authorship contribution statement

Mark A. Hughes: Conceptualization, Methodology, Writing – Original Draft. **Robert McMaster:** Investigation, Methodology, Writing – Review & Editing. **John E. Proctor:** Supervision, Methodology, Writing – Review & Editing. **Daniel W. Hewak:** Methodology, Writing – Review & Editing, Funding acquisition. **Takenobu Suzuki:** Methodology. **Yasutake Ohishi:** Methodology, Supervision.

Acknowledgements

The University of Southampton acknowledges the support of the Engineering and Physical Science Research Council through grant EP/M015130/1 Manufacturing and Application of Next Generation Chalcogenides.

Disclosure statement

No potential conflict of interest was reported by the author(s).

Funding

This work was supported by Engineering and Physical Sciences Research Council [grant number EP/M015130/1].

Data availability

The datasets generated during the current study are available in the Mendeley Data repository <http://dx.doi.org/10.17632/phrg25hv9j.1>.

ORCID

Mark A. Hughes  <http://orcid.org/0000-0002-0877-5279>

References

- [1] Hughes MA, Akada T, Suzuki T, et al. Ultrabroad emission from a bismuth doped chalcogenide glass. *Opt Express*. 2009;17(22):19345–19355.
- [2] Dianov EM, Dvoyrin V, Mashinsky VM, et al. CW bismuth fibre laser. *Quantum Electron*. 2005;35(12):1083.
- [3] Bufetov IA, Dianov EM. Bi-doped fiber lasers. *Laser Phys Lett*. 2009;6(7):487–504.
- [4] Shubin A, Bufetov I, Melkumov M, et al. Bismuth-doped silica-based fiber lasers operating between 1389 and 1538 nm with output power of up to 22 W. *Opt Lett*. 2012;37(13):2589–2591.
- [5] Firstov S, Alyshev S, Melkumov M, et al. Bismuth-doped optical fibers and fiber lasers for a spectral region of 1600–1800nm. *Opt Lett*. 2014;39(24):6927–6930.
- [6] Thipparapu NK, Wang Y, Wang S, et al. Bi-doped fiber amplifiers and lasers [invited]. *Opt Mater Express*. 2019;9(6):2446–2465.
- [7] Peng M, Qiu J, Chen D, et al. Superbroadband 1310 nm emission from bismuth and tantalum codoped germanium oxide glasses. *Opt Lett*. 2005;30(18):2433–2435.
- [8] Khonthon S, Morimoto S, Arai Y, et al. Luminescence characteristics of Te- and Bi-doped glasses and glass-ceramics. *J Ceram Soc Jpn*. 2007;115(1340):259–263.
- [9] Sokolov VO, Plotnichenko VG, Dianov EM. Origin of broadband near-infrared luminescence in bismuth-doped glasses. *Opt Lett*. 2008;33(13):1488–1490.
- [10] Sharonov MY, Bykov AB, Petricevic V, et al. Spectroscopic study of optical centers formed in Bi-, Pb-, Sb-, Sn-, Te-, and In-doped germanate glasses. *Opt Lett*. 2008 Sep;33(18):2131–2133.
- [11] Meng XG, Qiu JR, Peng MY, et al. Infrared broadband emission of bismuth-doped barium-aluminum-borate glasses. *Opt Express*. 2005;13(5):1635–1642.
- [12] Fujimoto Y, Nakatsuka M. Infrared luminescence from bismuth-doped silica glass. *Jpn J Appl Phys Part 2 Lett*. 2001;40:L279–L281.
- [13] Wang X, Xia H. Infrared superbroadband emission of Bi ion doped germanium-aluminum-sodium glass. *Opt Commun*. 2006;268(1):75–78.
- [14] Cao J, Xu S, Zhang Q, et al. Ultrabroad photoemission from an amorphous solid by topochemical reduction. *Adv Opt Mater*. 2018;6(22):1801059.
- [15] Hughes MA, Suzuki T, Ohishi Y. Compositional optimization of bismuth-doped yttria-alumina-silica glass. *Opt Mater*. 2009;32:368–373.
- [16] Suzuki T, Ohishi Y. Ultrabroadband near-infrared emission from Bi-doped $\text{Li}_2\text{O-Al}_2\text{O}_3\text{-SiO}_2$ glass. *Appl Phys Lett*. 2006;88(19):191912.
- [17] Hughes MA, Suzuki T, Ohishi Y. Compositional dependence of the optical properties of bismuth doped lead-aluminum-germanate glass. *Opt Mater*. 2010;32(9):1028–1034.
- [18] Proctor J, Massey D. Electric discharge machine for preparation of diamond anvil cell sample chambers. *Rev Sci Instrum*. 2018;89(10):105109.
- [19] Tateiwa N, Haga Y. Evaluations of pressure-transmitting media for cryogenic experiments with diamond anvil cell. *Rev Sci Instrum*. 2009;80(12):123901.
- [20] Goncharov AF, Zaug JM, Crowhurst JC, et al. Optical calibration of pressure sensors for high pressures and temperatures. *J Appl Phys*. 2005;97(9):094917.
- [21] Hakeem MA, Jackson DE, Hamlin JJ, et al. High pressure Raman, optical absorption, and resistivity study of SrCrO_4 . *Inorg Chem*. 2018;57(13):7550–7557.
- [22] Swart H, Kroon R. Ultraviolet and visible luminescence from bismuth doped materials. *Opt Mater X*. 2019;2:100025.
- [23] Hughes G, Suzuki T, Ohishi Y. Advanced bismuth doped lead-germanate glass for broadband optical gain devices. *J Opt Soc Am B*. 2008;25(8):1380–1386.
- [24] Van der Steen A, Van Hesteren J, Slok A. Luminescence of the Bi^{3+} Ion in Compounds LiLnO_2 and NaLnO_2 ($\text{Ln} = \text{Sc, Y, La, Gd, Lu}$). *J Electrochem Soc*. 1981;128(6):1327.
- [25] Blasse G. The ultraviolet absorption bands of Bi^{3+} and Eu^{3+} in oxides. *J Solid State Chem*. 1972;4(1):52–54.
- [26] Krasnikov A, Mihokova E, Nikl M, et al. Luminescence spectroscopy and origin of luminescence centers in Bi-doped materials. *Crystals (Basel)*. 2020;10(3):208.

- [27] Blasse G, Bril A. Investigations on Bi^{3+} -activated phosphors. *J Chem Phys.* **1968**;48(1):217–222.
- [28] Han J, Li L, Peng M, et al. Toward Bi^{3+} red luminescence with no visible reabsorption through manageable energy interaction and crystal defect modulation in single Bi^{3+} -doped ZnWO_4 crystal. *Chem Mater.* **2017**;29(19):8412–8424.
- [29] Bufetov IA, Melkumov MA, Firstov SV, et al. Bi-doped optical fibers and fiber lasers. *IEEE J Sel Top Quantum Electr.* **2014**;20(5):111–125.
- [30] Sun H-T, Zhou J, Qiu J. Recent advances in bismuth activated photonic materials. *Prog Mater Sci.* **2014**;64:1–72.
- [31] Dianov E. Nature of Bi-related near IR active centers in glasses: state of the art and first reliable results. *Laser Phys Lett.* **2015**;12(9):095106.
- [32] Laguta OV, El Hamzaoui H, Bouazaoui M, et al. On the nature of photoluminescence in bismuth-doped silica glass. *Sci Rep.* **2017**;7(1):1–6.
- [33] Suresh B, Purnachand N, Zhydachevskii Y, et al. Influence of Bi^{3+} ions on the amplification of 1.3 μm emission of Pr^{3+} ions in lead silicate glasses for the applications in second telecom window communications. *J Lumines.* **2017**;182:312–322.
- [34] Halder A, Kir'yanov A, Sekiya EH, et al. Fabrication and characterization of bismuth-doped germano-silicate and phospho-silicate fibers for VIS/NIR applications. *Opt Mater Express.* **2019**;9(4):1815–1825.
- [35] Halder A, Bhadra S K, Bysakh S, et al. Strong and broad visible emission of bismuth doped nano-phase separated yttria-alumina-silica optical fibers. *Curr Nanosci.* **2016**;12(3):309–315.
- [36] Sokolov V, Plotnichenko V, Dianov E. The origin of near-IR luminescence in bismuth-doped silica and germania glasses free of other dopants: first-principle study. *Opt Mater Express.* **2013**;3(8):1059–1074.
- [37] Hughes MA, Gwilliam RM, Homewood K, et al. On the analogy between photoluminescence and carrier-type reversal in Bi- and Pb-doped glasses. *Opt Express.* **2013**;21(7):8101–8115.
- [38] Peng M, Zollfrank C, Wondraczek L. Origin of broad NIR photoluminescence in bismuthate glass and Bi-doped glasses at room temperature. *J Phys Condes Matter.* **2009**;21(28):285106.
- [39] Wamsley P, Bray K. The effect of pressure on the luminescence of Cr^{3+} : YAG. *J Lumines.* **1994**;59(1-2):11–17.
- [40] Galanciak D, Perlin P, Grinberg M, et al. High pressure spectroscopy of LLGG doped with Cr^{3+} . *J Lumines.* **1994**;60:223–226.
- [41] Quérel G, Reynard B. High-pressure luminescence spectroscopy of transition elements: experimental setup and preliminary results on Cr^{3+} in silicate glasses. *Chem Geol.* **1996**;128(1–4):65–75.
- [42] Abu-Eid R, Burns R. The effect of pressure on the degree of covalency of the cation-oxygen bond in minerals. *Am Miner.* **1976**;61(5–6):391–397.
- [43] Bray KL. High pressure probes of electronic structure and luminescence properties of transition metal and lanthanide systems. *Transition metal and rare earth compounds*: Springer; Berlin Heidelberg, Ed. H. Yersin, 2001. p. 1–94.
- [44] Xue X, Stebbins JF, Kanzaki M, et al. Pressure-induced silicon coordination and tetrahedral structural changes in alkali oxide-silica melts up to 12 GPa: NMR, Raman, and infrared spectroscopy. *Am Miner.* **1991**;76(1-2):8–26.
- [45] Mahlik S, Amer M, Boutinaud P. Energy level structure of Bi^{3+} in zircon and scheelite polymorphs of YVO_4 . *J Phys Chem C.* **2016**;120(15):8261–8265.
- [46] Hughes MA, Fedorenko Y, Gholipour B, et al. N-type chalcogenides by ion implantation. *Nat Commun.* **2014**;5:5346.